ISSN 8755-6839

SCIENCE OF TSUNAMI HAZARDS

Journal of Tsunami Society International

Volume 40 Number 4 2021

SEISMIC WAVE PROPAGATION IN BANDUNG BASIN, WEST JAVA

Anggun Mayang Sari[1]; Afnindar Fakhrurrozi[1]; Arifan Jaya Syahbana[1,2]; Dwi Sarah[1]; Mudrik Rahmawan Daryono[1]; Bambang Setiadi [1]; Rabieahtul Abu Bakar[3]; Jian Cheng Lee[4,5]

[1]Research Centre for Geotechnology – National Research and Innovation Agency (BRIN), Jl. Sangkuriang Gd 70, Bandung 40135, Indonesia
[2]Faculty of Civil and Environmental Engineering, Bandung Institute of Technology, Bandung, Indonesia
[3]Razak Faculty of Technology and Informatics, University Technology Malaysia (UTM), Kuala Lumpur, Malaysia
[4]Institute of Earth Science, Academia Sinica, Taipei, Taiwan
[5]Integrated Research on Disaster Risk-International Centre of Excellence (IRDR-ICoE), Taipei, Taiwan
contact email: anggun.mayang.sari@brin.go.id; anggunnmayangsari@gmail.com

ABSTRACT

Wave propagation is a fundamental issue in all over seismic prone areas, including in the Bandung basin. Bandung basin consists of several geological formations. Based on the tectonic conditions, this area is surrounded by active seismic sources. Several main faults play a role part in dynamic soil conditions. Wave propagation from earthquake shaking has a significant impact on the soil surface. Recent studies in the Bandung basin showed the seismic hazard on the bedrock, but less understanding of hazard on the soil surface. Building construction failures caused by the soil surface's ground-shaking correlate linearly with the Peak Ground Acceleration (PGA) value. This paper discusses the soil surface acceleration on the Bandung basin using the wave propagation method using a non-linear seismic response analysis. The result shows that the highest soil surface acceleration is found in the Tanjung Jaya village, while the lowest is in Ciwastra village. The PGA value varies between 0.42g to 0.70 g. The seismic ground-motion strongly influences these results on bedrock and soil stratigraphy in the survey area.

Keywords: *wave propagation; Bandung basin; soil surface; ground-motion; PGA*

1. INTRODUCTION

The seismic hazard zone is an area that is at risk of experiencing the impact of earthquake events, such as landslides, liquefaction, building failure and human fatality. The seismic zone location is generally close to the seismic hazard zone, the seismic source focus. Nevertheless, many attractive tourism area locations are inside of the earthquake source (Orchiston, 2010). Some of these tourism places, such as Sianok Valley, located at Semangko fault line in West Sumatera and Lembang tourist area, settled down at the top of Lembang fault in West Java (Sieh et al., 2000; Novianti et al., 2021).

These areas then transformed entirely into densely populated area that urgently requires preparedness efforts for disaster risk reduction. The seismic event in Bandung basin occurred more frequently in the last two decades. The distribution of earthquake sources that affect seismicity in the Bandung Basin area is shown in Figure 1. Some of them have a more significant impact due to their location close to the Bandung Basin, namely Lembang Fault, Cimandiri Fault and Baribis Fault.

The Lembang Fault has a length of 29 km, stretches from Cipogor to Batu Lonceng area (Daryono, 2019). Moreover, the slip rate moves continuously by 1.95–3.45 mm/year. It also has magnitudes around Mw 6.5 – 7.0 with a recurrence time between 170-670 years. As for Cimandiri Fault is materialized in the form of a straight valley and hills that stretches from the west of Pelabuhan Ratu to the east of Mount Tangkuban Parahu (Haryanto et al., 2017). Meanwhile, The Baribis Fault is located in the eastern part of West Java, which stretches from the Subang area to Majalengka and Kuningan (Bemmelen, 1949).

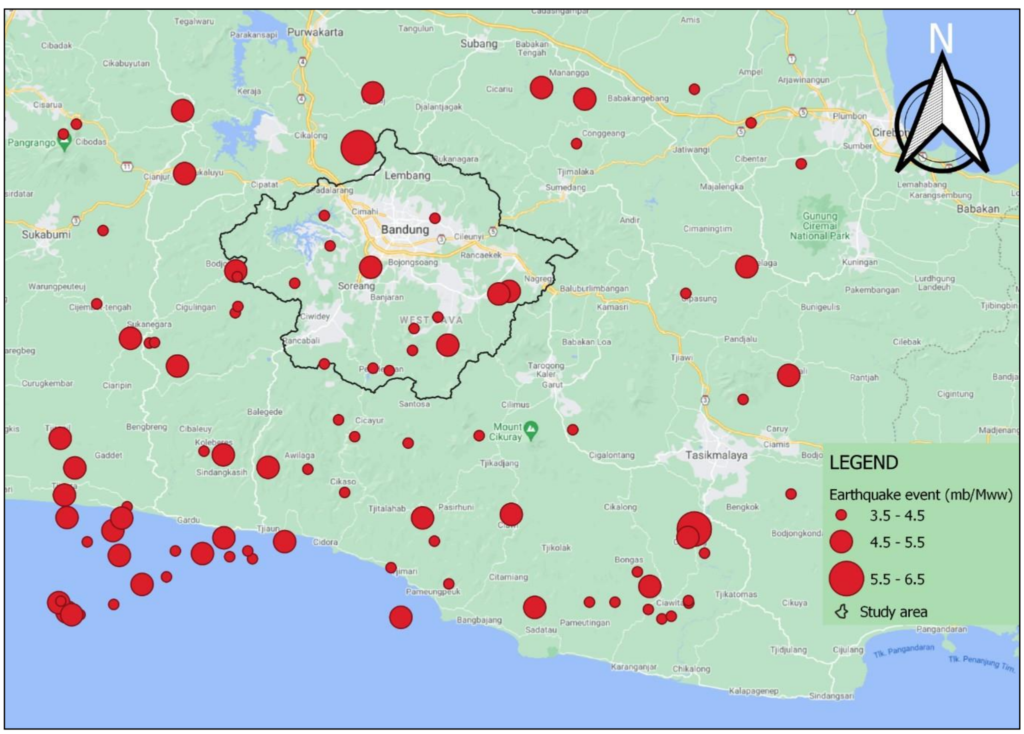

Figure 1. A series of earthquake events in the last 20 years in the surrounding Bandung basin (USGS., 2021).

Several major earthquakes have caused heavy losses of both property and life in the Bandung basin. One of the major earthquakes that involved significant damage was the Tasikmalaya earthquake on September 2, 2009, with an earthquake magnitude of 7.0 Mw in a depth of 46.2 km(Meilano et al., 2010). It caused 771 people to be injured, 23 people have died, and 75805 residents were evacuated (Badan Penanggulangan Bencana Nasional, 2009). Furthermore, it also caused heavy damage to physical infrastructure, around 15,538 residential houses were severely damaged, and 30,591 houses were slightly damaged (Pusat Data Informasi dan Komunikasi Kebencanaan, 2021).

In this study, we hypothesized that the earthquake wave on the soil surface has a significant correlation with the number of building failures and lives losses based on the existing dataset. Hence, we analyzed the seismic wave propagation from bedrock to soil surface using non-linear earthquake response analysis. Several vital factors in the study are ground-motion characterization at bedrock and geological interpretation on specific survey locations. The dynamic soil response on the surface quantity is shown from the PGA value.

2. GEOLOGICAL SETTING

Bandung city and its surroundings consist of a large intermountain basin surrounded by volcanic highlands. The central Bandung plain is situated at 665 m above sea level and is surrounded by up to 2400 m high Late Tertiary and Quaternary volcanic terrain (Dam et al., 1996). The Bandung basin is bounded by the Tangkuban Perahu volcanic complex, Mandalawangi Mount in the North to the East, and Patuha-Patuha-MalabarMalabar volcanic complex in the South. The Bandung basin is considered a graben-like depression controlled by geological structure and lithology, as shown in Table 1 (Delinom, 2009).

Table 1. The lithology of the Bandung basin (Hutasoit, 2009; Silitonga, 1973).

Formation	Remarks
Tertiary sedimentary and volcanic rocks	The Tertiary sedimentary and volcanic rocks are the oldest units of Late Miocene to Early Pliocene, widely exposed in the West Bandung.
Cikapundung Formation	Cikapundung Formation comprises the intercalation of volcanic breccia and conglomerates, lahar, and lava of Pleistocene age. This Formation lies unconformably on top of the Tertiary rocks. The Cikapundung Formation occupies the northern part the of Bandung basin.
Cibereum Formation	Cibereum Formation consists of a sequence of volcanic breccia and tuff deposits with some lava intrusion, is of Late Pleistocene to Holocene age. The Cibereum Formation and other Quartenary volcanic products from volcanic fans spreading from the northern and southern volcanic complexes to the centre of the basin

Kosambi Formation	Kosambi Formation is of the Holocene age, widely distributed in the centre of the Bandung Basin. Kosambi Formation consists of unconsolidated clay, organics, silt, and sandstone, also known as the lake deposit. This Formation is inter-fingering with the Cibereum Formation.

Major geological faults and lineaments in the study area are generally E-W, SW-NE, SE-NW oriented, and a few are oriented almost N-S (Figure 2) (Marjiyono et al., 2008). The E-W faults are the Lembang fault at the North and Gunung Geulis and Citarum faults at the South. SW-NE faults are the Cicalengka and Cileunyi-Tanjungsari faults, and the almost N-S fault is Bandasari fault; all these faults are left strike-slip faults. A conspicuous geomorphic ridge trending east-west of 29 km is observed in the North part of the Bandung basin, the Lembang active fault. Dam (1996) divided the Lembang fault segments into a normal fault in the western part and strike-slip in the East part. According to Daryono et al. (2018), the Lembang fault has predominantly sinistral movement capable of generating 6.5-7.0 Mw earthquake with a recurrence time of 170-670 years.

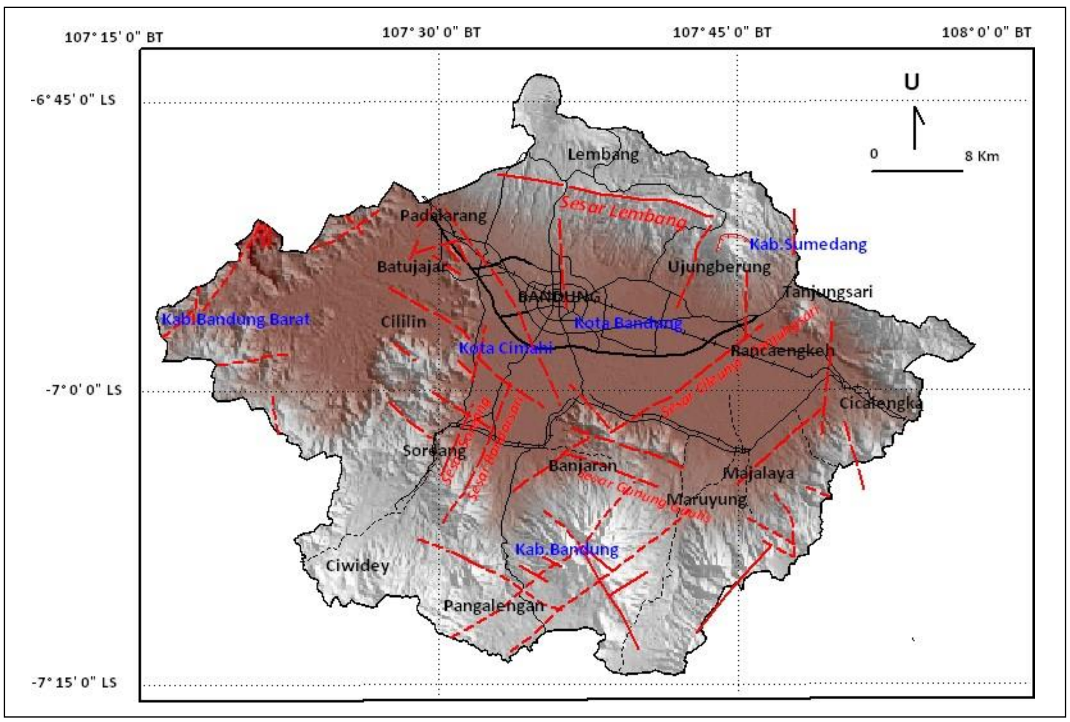

Figure 2. Geological Condition and Tectonic Setting of Bandung basin (compiled and modified from Silitonga (1973), Marjiyono (2008), Hutasoit (2009), Daryono (2018)).

The study locations spread on 35 soil investigation test locations in Bandung basin. The soil investigation test consists of the Cone Penetration Test unit (CPTu) and Bore Hole test (BH). These locations are distributed on several regencies in Bandung basin: Bandung City, Bandung regency, and West Bandung Regency. The distribution of survey point locations can be seen in Figure 3.

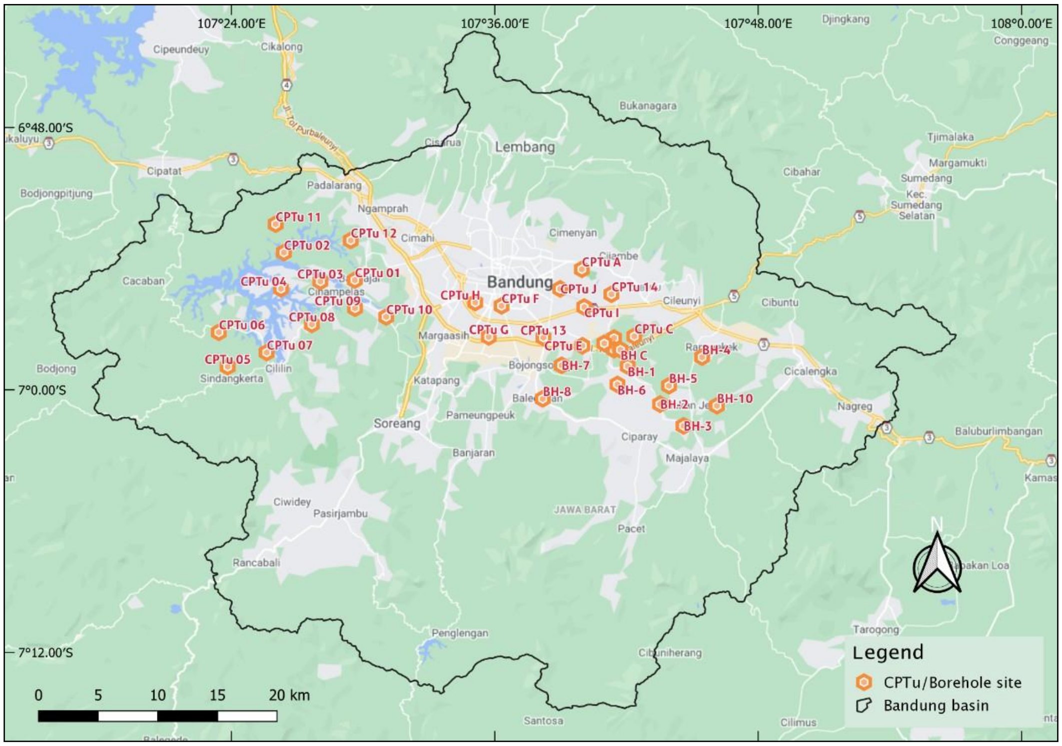

Figure 3. Study locations of wave propagation analysis in Bandung basin

3. METHODS

A. Ground Motion Synthetic (GMS) Modelling

The GMS. Modelling is a technique for generating the series event of acceleration, velocity or displacement concerning the function of time that correspond to ground motion modification in other locations (Gavin & Dickinson, 2011; Vlachos et al., 2018). There are several steps in the input data preparation before the GMS modelling. Firstly, the Probabilistic Seismic Hazard Analysis (PSHA) was used for the ground motion quantification at a particular location in a period of time. The PSHA computation also considers various earthquake mechanisms sources, which are faults, shallow to deep backgrounds, and megathrust. The earthquake source was determined using the logic tree of the Ground Motion Prediction Equation (GMPE). The 2017 Indonesia earthquake source mechanism compilation can be seen in Table 2 (Azwar et al., 2021; Irsyam et al., 2020; Sari et al., 2019; AJ Syahbana et al., 2021; Yuliastuti et al., 2021).

Table 2. The logic tree of GMPE.

No	Seismic Source	GMPE and Weighting
1	Active shallow crust (Fault and Shallow Background)	Boore Atkinson 2008 0.2 Campbell Bozorgnia 2008 0.2 Chiou Youngs 2008 0.2 Boore et al. 2014 0.133 Campbell Bozorgnia 2014 0.133 Chiou Youngs 2014 0.134

2	Subduction/Megathrust	Youngs et al. 1997 Sinter 0.15 Atkinson Boore 1995 GSC Best 0.15 Zhao et al. 2006 Sinter 0.30 Abrahamson et al 2015 Sinter 0.40
3	In slab Subduction (Deep Background)	Youngs et al 1997 SSlab 0.333 Atkinson Boore 2003 SSlab NSHMP 2008 0.333 Atkinson Boore 2003 SSlab Cascadia NSHMP 2008 0.334

Secondly, the de-aggregation or disaggregation technique was used to obtain the most dominant earthquake source in sequential time. Thirdly, earthquake records selection has parameters that are close to the result of the deaggregation. The equations are given by

$$M_{dominant} = \frac{\Sigma\, M_i\; x\; (\text{contribution of events/year})}{\Sigma\; (\text{contribution of events/year})} \tag{1}$$

$$R_{dominant} = \frac{\Sigma\, R_i\; x\; (\text{contribution of events/year})}{\Sigma\; (\text{contribution of events/year})} \tag{2}$$

With M is magnitude (Mw) and R is the distance (km). In this study, a synthetic ground motion was made using the EzFrisk software since no actual earthquake data recordings were available (Risk Engineering, 2011; A. Syahbana et al., 2019). The output of GMS will later be used in conducting further analysis, for example, wave propagation on the surface or as input for dynamic modelling of building structures.

B. Wave Propagation methods

Previous studies related to wave propagation of seismic motion on the surface have been accomplished using a similar algorithm (Scanlan, R. H. , 1976; Semblat et al., 2005; Semblat, J.F., 2011; Cheng et al., 2020). In contrast, Bardet and Tobita (2001) successfully developed a new algorithm for seismic wave propagation on the surface. It consists of non-linear elements to model soil behavior as the repercussions of earthquake waves. This algorithm is manifested into an application known as Nonlinear Earthquake Response Analysis (NERA). The main parameters of NERA are stress-strain, velocity, amplification by considering material models such as linear equivalent models, viscoelastic models and material models.

The first stage in the NERA modelling is an initialization, followed by the strain increment, strain andstress computation that is given by:

$$\gamma_{i,n} = \frac{d_{i+1,n} - d_{i,n}}{\Delta\, z_i} \tag{3}$$

$$\tau_{i,n} = IM(\tau_{i,n-1}, \Delta\, \gamma_{i,n} \tag{4}$$

Where $\gamma_{i,n}$, $\tau_{i,n}$, $d_{i,n}$, and z_i are the strain, the stress, displacement and thickness at node i (1, ..., n) respectively. NERA modelling use IM model to simulate non-linear stress-strain curves. The second stage of NERA modelling is to compute the velocity that is given by:

$$V_{i,n} = V_{i,n-1} + \frac{1}{2}(a_{i,n} + a_{i,n-1})\,\Delta t \tag{5}$$

Where $V_{i,n}$, $a_{i,n}$ are the velocity and the acceleration at node i (1, ..., n) and time respectively. The predicted velocity at time t_n and t_{n+1} can be obtained using $V_{i,n}$ and the Newmark algorithm is given by:

$$\tilde{v}_{N,n+1} = \frac{\tilde{v}_{N,n}(\Delta z_{N-1} - v_s \Delta t) + 4v_s V_{i,n} \Delta t - 2\tau_{N-1,n} \frac{\Delta t}{\rho_N}}{\Delta z_{N-1} + v_s \Delta t} \tag{6}$$

Where $\tilde{v}_{N,n+1}$ is predicted velocity at N grid and n (n, …., n+1) sequence, is depth, and is unit mass. The final step in NERA modelling is to compute displacement (*d*), velocity ( ) and acceleration ( ) using equations on each parameter, given by:

$$d_{i,n+1} = d_{i,n} + \tilde{v}_{i,n+1}\,\Delta t \tag{7}$$

$$v_{i,n} = \frac{1}{2}(\tilde{v}_{i,n+1} + \tilde{v}_{i,n}) \tag{8}$$

$$a_{i,n} = \frac{1}{2}(\tilde{v}_{i,n+1} + \tilde{v}_{i,n}) \tag{9}$$

The result of wave propagation from bedrock to the ground surface computation can be acquired from the highest acceleration value, as shown in Figure 4. The main parameters as input data in the NERA modelling that need attention are ground motion data in the bedrock and soil layer data. The ground motion data is the earthquake input motion data that was acquired from the ground-motion synthetic modelling. While the soil layer data were obtained from the soil field investigation test data, namely the cone penetration test and the borehole test.

C. Amplification factors

The amplification factor is a ratio of peak ground acceleration on bedrock to peak ground accelerationon the soil surface (Horri et al., 2019). The equation for calculation amplification factor is given by:

$$F_{PGA} = \frac{PGA_{surface}}{PGA_{bedrock}} \tag{10}$$

Where $PGA_{surface}$ is peak ground acceleration based on wave propagation calculation (g), and $PGA_{bedrock}$ is peak ground acceleration based on ground motion at bedrock (g).

The amplification factor was applied to validate the amplification factor from the previous calculation using site class coefficients. The amplification factor was determined using site coefficient FPGA from ASCE 7-10, as shown in Table 3.

Table 3. F_{PGA} Site Class Coefficient.

Site Class	Peak ground acceleration adjusted from site class				
	PGA≤0.1	PGA=0.2	PGA=0.3	PGA=0.4	PGA≥0.5
A	0.8	0.8	0.8	0.8	0.8
B	1.0	1.0	1.0	1.0	1.0
C	1.2	1.2	1.1	1.0	1.0
D	1.6	1.4	1.2	1.1	1.0
E	2.5	1.7	1.2	0.9	0.9
F	See section 11.4.7				

The site class of study locations were determined using ASCE 7-05 Site Class Definitions. The CPTu and borehole data are collected to analyze the average standard penetration resistance ($\bar{N}$). After calculating $\bar{N}$ value, the site class of certain point locations can be defined using Table 4.

Table 4. Site Class Definitions from ASCE 7-05.

Site Class	Site Profile Name	Soil Shear Wave Velocity, $\bar{V}_s$ (ft/sec)	Standard Penetration Resistance, $\bar{N}$	Undrained Shear Strength, $\bar{S}_u$ (psf)
A	Hard rock	$\bar{V}_s$ > 5,000	NA	NA
B	Rock	2,500 < $\bar{V}_s$ ≤ 5,000	NA	NA
C	Very dense soil and soft rock	1,200 < $\bar{V}_s$ ≤ 2,500	> 50	> 2,000 psf
D	Stiff soil	600 < $\bar{V}_s$ ≤ 1,200	15 to 20	1,000 to 2,000 psf
E	Soft clay soil	$\bar{V}_s$ ≤ 600	< 15	< 1,000 psf
		Any profile with more than 10 ft of soil having the following characteristics: • Plasticity index PI> 20 • Moisture content ω ≥ 40%, and • Undrained shear strength S_u < 500 psf		
F	Soil requires site response analysis	Liquefiable soils, peat, high plasticity clay		

4. RESULTS AND DISCUSSION

A. GMS on Bedrock

The dominant seismic sources resulting from the GMS modelling on bedrock are earthquakes originating from Lembang Fault and West Central Java Megathrust. The maximum acceleration values were obtained by performing spectral matching on dominant M and R. The results of GMS modelling as shown in Table 5.

Table 5. Ground motion acceleration on bedrock ($PGA_{bedrock}$)

Point Location	a_{max} (g)	Point Location	a_{max} (g)	Point Location	a_{max} (g)	Point Location	a_{max} (g)	Point Location	a_{max} (g)
BH-01	0.50	BH-08	0.52	CPTu-06	0.53	CPTu-13	0.46	CPTu-D	0.48
BH-02	0.51	BH-10	0.50	CPTu-07	0.51	CPTu-14	0.50	CPTu-E	0.48
BH-03	0.49	CPTu-01	0.58	CPTu-08	0.53	BH-A	0.49	CPTu-F	0.49
BH-04	0.55	CPTu-02	0.60	CPTu-09	0.51	BH-B	0.49	CPTu-G	0.50
BH-05	0.49	CPTu-03	0.52	CPTu-10	0.54	BH-C	0.49	CPTu-H	0.53
BH-06	0.51	CPTu-04	0.69	CPTu-11	0.69	CPTu-A	0.62	CPTu-I	0.50
BH-07	0.54	CPTu-05	0.52	CPTu-12	0.67	CPTu-C	0.51	CPTu-J	0.51

The peak ground acceleration on bedrock (PGAbedrock) value varies from 0.46g to 0.69g. The maximum acceleration found on CPTu-04, which is located at Tanjung Jaya village, West Bandung Regency. The PGAbedrock value is around 0.69g, heavily influenced by Lembang fault mechanism, based on deaggregation analysis. The point location is closed to Lembang fault. Meanwhile, the minimum acceleration value on bedrock found on CPTu-13, around 0.46g. This point location is located at Buah Batu district, Bandung City. From the deaggregation analysis result, the ground-motion acceleration is affected by the West-Central Java Megathrust mechanism.

B. Peak Ground Acceleration on Surface

After calculating the GMS on bedrock, the next step to estimating PGA on the ground surface. It is to interpret the soil layer profile. The soil layer profile was obtained from the CPTu test and BH test. The cross-section from the Northwest (NW) to the Southeast (SE) of Bandung basin, as shown in Figure 4. Clay deposits dominate the soil properties, while some organic soils are found in the middle of soil depth. The sand soils are distributed at the thin layer over the section and become thicker at the bottom of the soil depth. Difference to NW-SE section, the Northeast (NE) to southwest (SW) cross-section has the heterogeneity of soil deposit, as shown in Figure 5. The organic soil and clay to silty clay soil are found at 35 meters of soil thickness. The volcanic breccia was also found at CPTu-G to CPTu-H cross-section. The hard soil settles down from 601 to 641 meters above sea level, consisting of silt soil and granular sand soil. The altered volcanic breccia lay down at 601 meters above sea level, located under the granular soil layer.

The soil profile and GMS data were used as input in surface soil acceleration modelling. The soil profile uses geological interpretation data from soil investigation tests. The results of the PGA on the surface analysis in Bandung basin area can be seen in Figure 6.

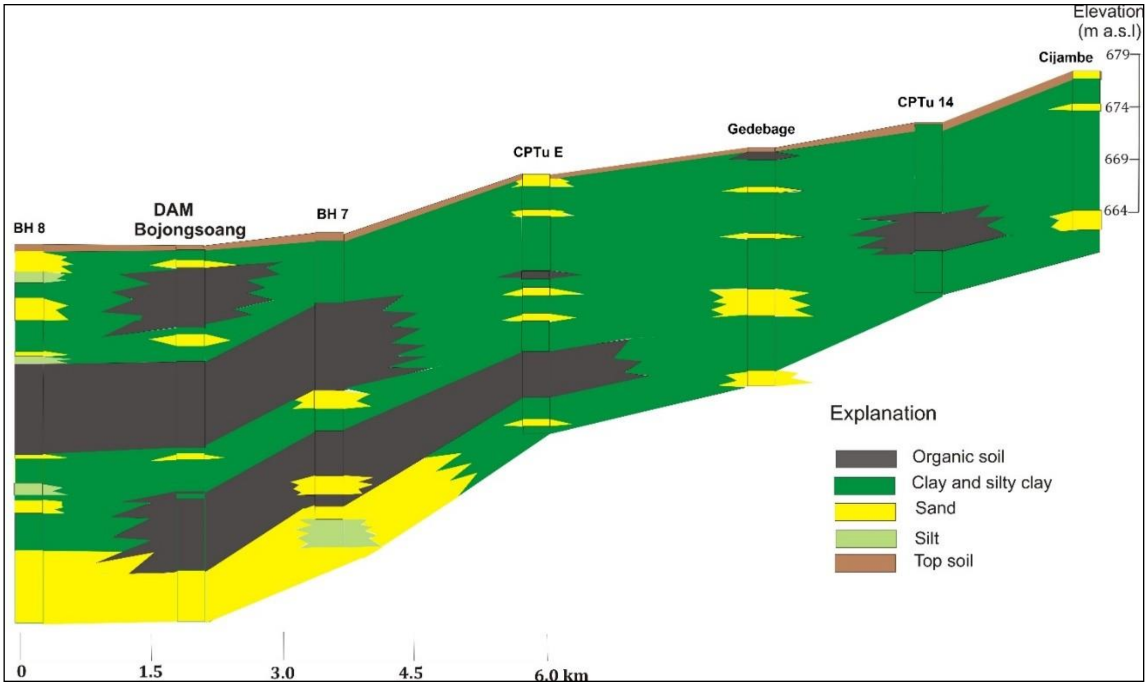

Figure 4. Cross section of Bandung basin from NE – SW

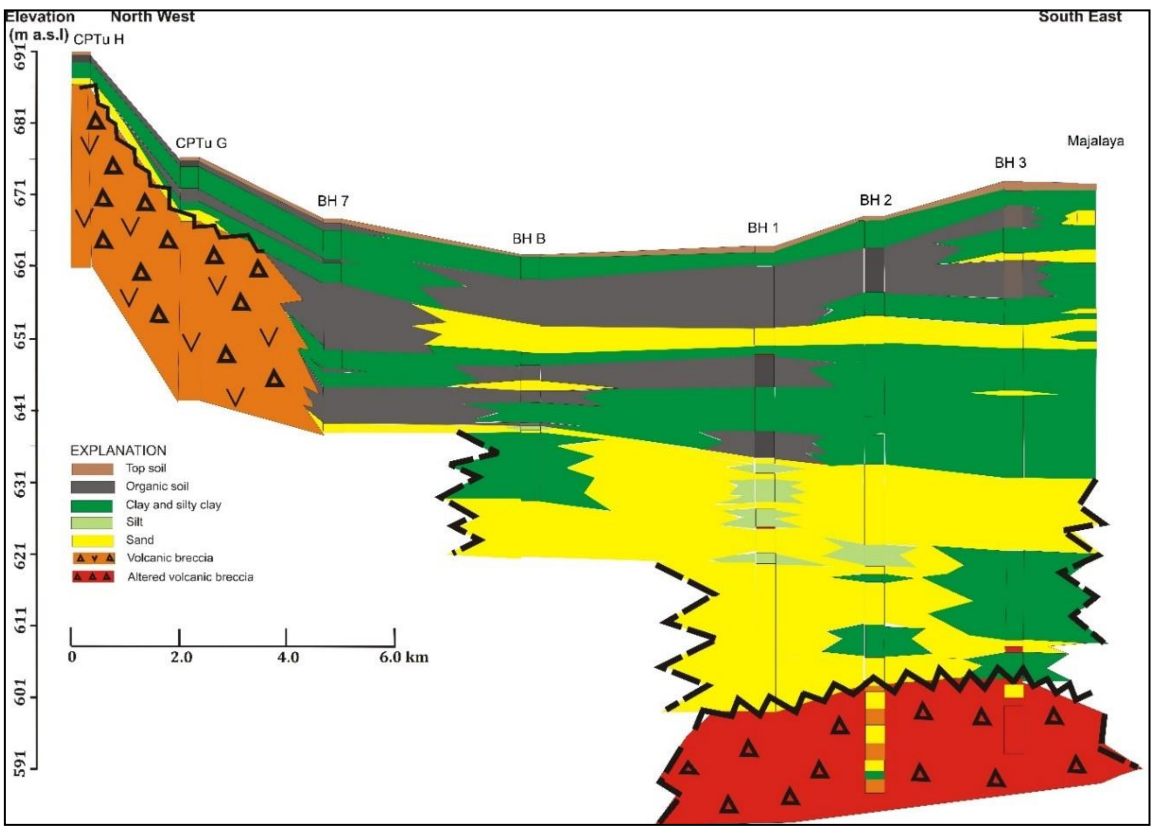

Figure 5. Cross section of Bandung basin from NW – SE

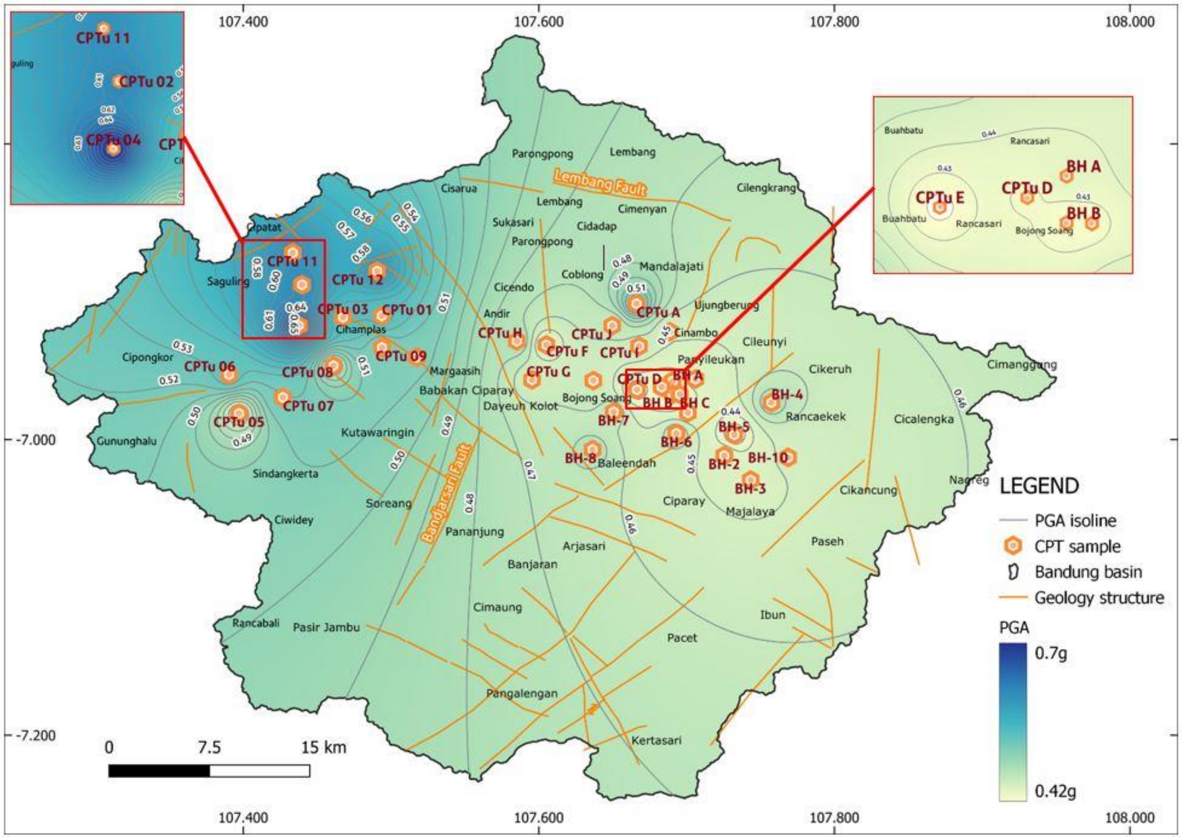

Fig. 6. Seismic Wave Propagation Map using $PGA_{surface}$ value on Bandung basin

Based on wave propagation analysis from bedrock ground-motion to the soil surface, the maximum PGA on the ground surface (a_{max},surface) is found at CPTu-04, which is located at Tanjung Jaya village, West Bandung regency. The result shows a value of 0.70g. The surface acceleration value is strongly influenced by stiff soil deposits that consist of silt soil and sand soil in 20 meters depth based on Cone Penetration Test data. This result is also affected by the ground- motion analysis at bedrock, where the bedrock acceleration value is relatively high, which is about 0.69g. The geological lithology on this location consists of tertiary sedimentary rocks. Besides, the tectonic condition plays a vital role in the bedrock acceleration since Lembang Fault is closed to this location.

Unlike Tanjung Jaya village, the minimum PGA value on the soil surface is found at Ciwastra village, Bandung City. The CPTu-E is located in this area. The surface acceleration value is around 0.42g. This value is affected by the soft soil deposit obtained 25 meters deep using the Cone Penetration Test. The soft soil deposit is dominated by clay soil and silt soil.

In contrast to the CPTu-04 case, the bedrock acceleration on CPTu-E is higher than the soil surface acceleration. The bedrock acceleration showed a value of 0.48g, while the soil surface acceleration presented a 0.42g value. The de-amplification phenomenon is happened in this location due to the thick, soft soil conditions (Villalobos et al., 2019; Midorikawa et al., 2014).

C. Amplification Factors

The ratio of amplification factor using PGA bedrock to PGA surface values can be seen in Table 6. The table presents the amplification factors (FPGA) value that varies from 0.9 to 1.0. Most of the area on Bandung regency and a few parts of Bandung City has an FPGA value is 0.9. From the cross-section of NW-SE and NE-SW, these locations are formed by soft soil deposits. These areas also lay down on the top of Kosambi formation, which is consists of clay, organics, silt, and sandstone.

In contrast to these locations, the West Bandung regency is dominated by stiff soil consisting of sand, silt, and rock formation. The FPGA value is 1.0. These locations settle down at the Cibereum Formation, tertiary sedimentary and volcanic rocks formation consisting of volcanic breccia and tuff deposits.

Validation of the amplification factor using dataset resulting from calculation to the amplification factor using site class coefficient, as shown in Table 7. The site class of 35 study locations in Bandung basin is also presented in this table. From this table, the site class E provides in Bandung regency and a few areas of Bandung City. Meanwhile, site class D shows some parts of West Bandung regency, which is CPTu-02, 03, 04, 07, 09 and CPTu-13 at Bandung City. Site class C remarkably is found at CPTu-06, which is located at West Bandung regency. The soil profile data shows that this point location consists of silt, sand and gravelly sand. Moreover, the data shows hard soil from 8 meters below.

After determining the site classification, the FPGA was estimated using the site class coefficient as depicted in Table 3. The PGA value is obtained from PGAbedrock value as depicted in Table 5 and interpolated to the FPGA value based on each site class determination. The FPGA from the site class coefficient can be seen in Table 6. It also presents the amplification and de-amplification phenomenon of each point location.

Table 6. F_{PGA} versus F_{PGA} using Site Class Coeff.

Point Location	$PGA_{bedrock}$ $a_{max,}$ (g)	$PGA_{surface}$ $a_{max,}$ (g)	F_{PGA}	Site Class	F_{PGA} (Site Class)	Amplification
BH-01	0.502	0.446	0.9	E	0.9	deamplification
BH-02	0.505	0.448	0.9	E	0.9	deamplification
BH-03	0.489	0.445	0.9	E	0.9	deamplification
BH-04	0.545	0.479	0.9	E	0.9	deamplification
BH-05	0.490	0.418	0.9	E	0.9	deamplification
BH-06	0.510	0.475	0.9	E	0.9	deamplification
BH-07	0.538	0.469	0.9	E	0.9	deamplification
BH-08	0.520	0.478	0.9	E	0.9	deamplification
BH-10	0.500	0.451	0.9	E	0.9	deamplification
CPTU01	0.578	0.544	0.9	E	0.9	deamplification
CPTU02	0.596	0.616	1.0	D	1.0	amplification
CPTU03	0.518	0.538	1.0	D	1.0	amplification
CPTU04	0.695	0.698	1.0	D	1.0	amplification
CPTU05	0.517	0.448	0.9	E	0.9	deamplification
CPTU06	0.526	0.537	1.0	C	1.0	amplification
CPTU07	0.509	0.520	1.0	D	1.0	amplification
CPTU08	0.525	0.467	0.9	E	0.9	deamplification
CPTU09	0.509	0.509	1.0	D	1.0	amplification
CPTU10	0.543	0.511	0.9	E	0.9	deamplification
CPTU11	0.677	0.607	0.9	E	0.9	deamplification
CPTU12	0.668	0.603	0.9	E	0.9	deamplification
CPTU13	0.457	0.456	1.0	D	1.0	amplification
CPTU14	0.499	0.449	0.9	E	0.9	deamplification
CPTU A	0.621	0.535	0.9	E	0.9	deamplification
CPTU C	0.506	0.447	0.9	E	0.9	deamplification
CPTU D	0.481	0.428	0.9	E	0.9	deamplification
CPTU E	0.483	0.417	0.9	E	0.9	deamplification

CPTU F	0.486	0.435	0.9	E	0.9	deamplification
CPTU G	0.500	0.451	0.9	E	0.9	deamplification
CPTU H	0.532	0.480	0.9	E	0.9	deamplification
CPTU I	0.497	0.458	0.9	E	0.9	deamplification
CPTU J	0.512	0.459	0.9	E	0.9	deamplification
BH A	0.488	0.440	0.9	E	0.9	deamplification
BH B	0.492	0.420	0.9	E	0.9	deamplification
BH C	0.488	0.426	0.9	E	0.9	deamplification

As seen in Table 5, the FPGA values are almost similar to the FPGA value using the site class coefficient. These values have a strong correlation to the properties of the soil layer. The stiff soil tends to have a high amplification factor, while the soft soil has a lower value. Moreover, the amplification and deamplification characteristics are influenced by the soil deposit. The amplification occurs in the hard soil layer in Site Class C and D, while deamplification occurs in the soft soil layer in Site Class E.

5. CONCLUSIONS

The wave propagation method is one of the procedures to estimate the seismic hazard on the ground surface. The PGA on the soil surface was obtained through several steps, including modelling ground-motion at the bedrock and characterizing the soil layer properties. The results show that the low potential seismic hazard occurs predominantly in Bandung regency and the eastern part of Bandung City. The site class calculation shows that these locations are strongly influenced by soft soil deposit, which is dominated by Site Class E. Meanwhile, the West Bandung regency has a high potential of ground shaking hazard, shown by the high PGA on the surface values. These conditions are affected by stiff soil deposits, presented from Site Class C and D determination.

The distance and magnitude of seismic sources to the point locations also significantly contribute to the acceleration calculation. From the deaggregation analysis, the western part and northern part of Bandung basin is influenced by Lembang fault. In contrast, the southern part and eastern part is affected by West-Central Java Megathrust mechanism. These whole analyses, from modelling the synthetic ground motion, interpreting the soil layer profile, and calculating the site classification, provide a systematic analysis of seismic hazard prediction. Future research direction needs to develop a complete stages computation and also consider the other parameters such as the effect of basin form on the surface acceleration and determining many soil properties uncertainties. Nonetheless, this research can provide basic earthquake mitigation information to deliver preliminary studies to estimate earthquake-resistant buildings through numerical and computational procedures.

AUTHOR CONTRIBUTIONS

Anggun Mayang Sari was in charge of conceptualization, design of methodology, data processing and manuscript writing – original draft and finishing. **Afnindar Fakhrurrozi** was in charge in both spatial and non-spatial data collection and curation, geospatial modelling and analysis, validation, data visualization and manuscript writing – original draft, review and editing. **Arifan Jaya Syahbana** was in charge of investigation, validation and manuscript writing - editing. **Dwi Sarah** was in charge of investigation, geological data analysis and manuscript writing - editing. **Mudrik Rahmawan Daryono** was in charge of investigation, seismic data resources. **Bambang Setiadi** was in charge of investigation. **Rabieahtul Abu Bakar** was in charge of manuscript writing – review. **Jian Cheng Lee** was in charge of supervision the project and provided financial support for the project leading to this publication.

ACKNOWLEDGMENT

This work was supported by the Research Incentive of National Innovation System (INSINAS)[grant number:10/INS/PPK/E4/2021] and the International Science Council Regional Office implements for Asia and the Pacific (ISC ROAP) and Integrated Research on Disaster Risk and the International Centre of Excellence Taipei (IRDR ICoE-Taipei) [the Advanced Institute Seed Grant Program, grant number:2G6G7Y4A].

REFERENCES

American Society of Civil Engineers (ASCE) 7-05. (2005). Minimum Design Loads for Buildings and Other Structures. Published by American Society of Civil Engineers, USA.

American Society of Civil Engineers (ASCE) 7-10. (2010). Minimum Design Loads for Buildings and Other Structures. Published by American Society of Civil Engineers, USA.

Azwar, C., Syahbana, A., Sari, A., Irsyam, M., Pamumpuni, A., and Sadisun, I. (2021). The Sensitivity of Maximum Magnitude Range Parameter in Bedrock Acceleration Calculation for 2500 Years of Return Period, Case Study: Bengkulu Province, Indonesia. 832(1), 012006.

Badan Nasional Penanggulangan Bencana (BNPB) (2009) Laporan Harian dari Pusdalops BNPB. 15 September 2009. Website www.bnpb.go.id.

Bardet, J.P and Tobita, T. (2001). A Computer Program for Nonlinear Earthquake site Response Analyses of Layered Soil Deposits. Manual Program. University of Southern California. Department of Civil Engineering.

Cheng, H., Luding, S., Saitoh, K., and Magnanimo, V. (2020). Elastic wave propagation in dry granular media: Effects of probing characteristics and stress history. International Journal of Solids and Structures 187 (2020) 85–99.

Dam, M.A.C., Suparan, P., Nossin, J.J., Voskuil, RPGA, Group, GTL (1996): A chronology for geomorphological developments in the greater Bandung area , West-Java, Indonesia. J. Southeast Asian Earth Sci. 14, 101–115.

Daryono, M. R., Natawidjaja, D.H., Sapiie, B. and Cummins, P. (2019): Earthquake Geology of the Lembang Fault, West Java, Indonesia. Tectonophysics,751, 180–191.

Delinom, R.M. (2009) : Structural geology controls on groundwater flow: Lembang Fault case study, West Java, Indonesia. Hydrogeol. J. 17, 1011–1023. https://doi.org/10.1007/s10040-009-0453-z

Gavin, H. P., & Dickinson, B. W. (2011). Generation of uniform-hazard earthquake ground motions. Journal of Structural Engineering, 137(3), 423–432.

Haryanto, I., Hutabarat, J., Sudradjat, A., Ilmi, N.N.,and Sunardi, E. (2017): Tektonik Sesar Cimandiri, Provinsi Jawa Barat. Bulletin of Scientific Contribution, 15, 3, 255 – 274.

https://dibi.bnpb.go.id/xdibi/read/7666/32/04/108/2009//2//1

https://www.usgs.gov/natural-hazards/earthquake-hazards/lists-maps-and-statistics

Horri, K., Mousavi, M., Motahari, M., and Farhadi, A. (2019). Modelling and studying the impact of soil plasticity on the site amplification factor in ground motion prediction equations. Journal of Seismology, 23, 1179–1200.

Hutasoit, L.M. (2009) : Kondisi Permukaan Air Tanah dengan dan tanpa peresapan buatan di daerah Bandung : Hasil Simulasi Numerik. J. Geol. Indones. 4, 177–188.

Irsyam, M., Cummins, P. R., Asrurifak, M., Faizal, L., Natawidjaja, D. H., Widiyantoro, S., Meilano, I., Triyoso, W., Rudiyanto, A., Hidayati, S., Ridwan, M., Hanifa, N. R., and Syahbana, A. J. (2020). Development of the 2017 national seismic hazard maps of Indonesia. Earthquake Spectra, I(25), 25. https://doi.org/10.1177/8755293020951206

Marjiyono, Soehaimi, A., Karnawan. (2008): Identifikasi Sesar Aktif Daerah Cekungan Bandung Dengan Citra Landsat dan Kegempaan. J. Sum XVIII, 81–88.

Meilano, I., Abidin, H. Z, Andreas, H., Anggreni, D., Gumilar, I., Kato, T., Harjono, H., Zulfakriza, Dewi, O., Agustan, and Arif Rahman. (2010). Pergeseran koseismik dari Gempa Bumi Jawa Barat 2009. Jurnal Lingkungan dan Bencana Geologi, Vol. 1 No. 1 April 2010: 35 – 42.

Midorikawa, S. Miura, E H., Atsumi, T. (2014). Characteristics of strong ground motion from the 2011 gigantic Tohoku, Japan earthquake, International Symposium for CISMID. 25th Aniversary.

Novianti, E., Endayana, C., Lusiana, E., Wulung, S.R. and Desiana, R. (2021): Persuasive Communication: Disaster Literacy in Tourism Areas. Review of International Geographical Education (RIGEO),11(4), 1203-1210.

Orchiston, C.H.R. (2010): Perceptions, preparedness and resiliencein the zone of the Alpine Fault,Southern Alps,New Zealand. University of Otago, Dunedin, New Zealand. 342 p.

Pusat Data Informasi dan Komunikasi Kebencanaan (Pusdatinkom) Badan Nasional Penanggulangan Bencana (BNPB). (2021).

Risk Engineering, I. (2011). EZ-FRISK (7.52).

Sari, A. M., Fakhrurrozi, A., and Syahbana, A. J. (2019). Peak Ground Acceleration on Bedrock using Probability Seismic Hazard Analysis Methods in Bandung City. Proceedings of the Proceedings of the 7th Mathematics, Science, and Computer Science Education International Seminar, MSCEIS.

Scanlan, R.H. (1976). Seismic Wave Effects on Soil-Structure Interaction. Earthquake Engineering And Structural Dynamics, Vol. 4, 379-388.

Semblat, J.F., Kham, M., Parara, E., Bard, P.Y., Pitilakis, K., Makra, K., Raptakis, D. (2005). Seismic wave amplification: Basin geometry vs soil layering. Volume 25, 7–10, 529-538.

Semblat, J.F. (2011). Modeling Seismic Wave Propagation and Amplification in 1D/2D/3D Linear and Nonlinear Unbounded Media. International Journal of Geomechanics. Volume 11, 6, December 2011.

Sieh, K. and Natawidjaja, D.H. (2000): Neotectonicosf the Sumatran fault, Indonesia. Journal Of Geophysical Research, 105, 295-28.

Silitonga, P.H. (1973): Peta Geologi Bandung.

Syahbana, A. J., Iqbal, P., Irsyam, M., Asrurifak, M., and Hendriyawan, H. (2021). Smoothed Gridded Seismicity Effect for Land-Use Development, Case Study: Kalimantan Island, Indonesia. Rudarsko-Geološko-Naftni Zbornik, 36(3), 115–126.

Syahbana, A., Sari, A. M., Soebowo, E., Irsyam, M., Hendriyawan, H., & Asrurifak, M. (2019). The sensitivity of earthquake input motion correlation with arias intensity and amplification, case study: Yogyakarta Special Region. 1280(2), 022069.

Van Bemmelen, R. W. (1949): The Geology of Indonesia. Vol. IA, Government Printing Office, Martinus Nijhof, The Hague. Netherlands.

Villalobos, M.A and Romanel, C. (2019). Seismic Response of a Soft Soil Deposit Using Non-Linear and Simplified Models. Proceedings of the VII ICEGE 7th International Conference on Earthquake Geotechnical Engineering. Rome, Italy, 17-20 June 2019.

Vlachos, C., Papakonstantinou, K. G., & Deodatis, G. (2018). Predictive model for site specific simulation of ground motions based on earthquake scenarios. Earthquake Engineering & Structural Dynamics, 47(1), 195–218.

Yuliastuti, Y., Syaeful, H., Syahbana, A. J., Alhakim, E. E., & Sembiring, T. M. (2021). One dimensional seismic response analysis at the non-commercial nuclear reactor site, Serpong—Indonesia. Rudarsko-Geološko-Naftni Zbornik (The Mining-Geological-Petroleum Bulletin), 36(2), 1–10. https://doi.org/10.17794/rgn.2021.2.1